



Total radiative heat loss and radiation distribution of liquid pool fire flames



Liang Zhou^a, Dong Zeng^{b,*}, Dongyang Li^a, Marcos Chaos^b

^a Chinese People's Armed Police Academy, Department of Fire Protection Engineering, 220 Xichang Rd, Langfang, Hebei 065000, People's Republic of China

^b FM Global, Research Division, 1151 Boston-Providence Turnpike, Norwood, MA 02062, USA

ARTICLE INFO

Keywords:

Pool fire
Radiative power distribution
Radiation fraction
Multiple-point source radiation model

ABSTRACT

The radiative characteristics of laboratory-scale pool fire flames have been studied in detail. Experiments were conducted in the ASTM E2058/ISO 12136 Fire Propagation Apparatus (FPA). Eleven liquid fuels with different sooting propensities, including alcohols and alkanes, burning in a 9.5 cm diameter quartz dish were considered. Radiative power distribution (along the flame axis) and global radiant emission were measured for all the fuels by using slit and wide-view-angle radiometers, respectively. The effects of measurement location and fuel type on the measured data were investigated. Radiation distribution profiles for a given fuel, when adequately normalized, show little sensitivity to the horizontal separation distance of the slit radiometer. Fuels with similar chemical structures exhibit similar distributions, consistent with flame image analyses. The radiative power distributions along with the wide-view-angle radiometer data were used to derive radiant fractions for the pool fires studied by applying a multiple-point source (MPS) radiation model. To examine the sensitivity of the calculated radiant fractions to the measurement location, the position of the wide-view-angle radiometer was considerably varied both vertically and horizontally. The results show that the radiant fractions derived based on the measured radiative power distribution are independent of the location of the wide-view-angle radiometer and consistent with literature values. Therefore, the approach developed in this study presents a flexible methodology apt for the accurate determination of radiation properties of diffusion flames in a laboratory setting.

1. Introduction

Radiation is the dominant heat transfer mode in fires of considerable scale [1] and it plays an important role in fire growth and spread mechanisms. Understanding the radiative characteristics of fires provides a fundamental basis for fire growth modeling [2]. One such characteristic is the radiant fraction (χ_r), defined as the ratio of the radiative power (\dot{Q}_r) to the theoretical heat release rate (\dot{Q}):

$$\chi_r = \frac{\dot{Q}_r}{\dot{Q}} \quad (1)$$

where \dot{Q} can be expressed as the product of the mass burning rate, \dot{m} , and the net calorific value of the fuel, ΔH_{cn}^0 . For jet flames, some studies showed that radiant fraction can be affected by the jet exit velocity [3,4] and/or the flame residence time [5,6]. On the other hand, it is generally accepted that for buoyant turbulent diffusion flames, which are relevant to fires, the radiant fraction is fuel specific and remains relatively constant over a range of combustion conditions [7–12].

Since the total radiative power, \dot{Q}_r , cannot be easily measured, a common practice is to measure the incident radiation at one location

near the fire, and then derive the total radiative power using a model. The accuracy of the derived radiant fraction is therefore affected by the model. The most widely used approach, due to its simplicity, is the single point source (SPS) model [13]. In this model, the flame is approximated by a point usually located at the centroid of the flame and the radiation from the point source is assumed to be isotropic. Then, \dot{Q}_r can be calculated from the following equation:

$$\dot{q}_g'' = \frac{\dot{Q}_r \tau}{4\pi S^2} \cos \phi \quad (2)$$

where \dot{q}_g'' is the heat flux measured by a gage (e.g., a radiometer) at a distance S from the point source, ϕ is the angle formed by the normal to the gage surface and the line of sight to the point source, and τ is the atmospheric transmissivity over the distance S .

The nature of the SPS model makes it only applicable to measurements performed in the far field of a given fire. Modak [13] showed that the radiative power output (and, thus, χ_r) of pool fires derived from the SPS model underestimated the true value by over 25% for measurements taken within one pool radius of the fire; such estimates improved considerably for measurements taken beyond ten pool radii. Hamins et al. [14] found that the SPS model yielded radiant fractions accurate

* Corresponding author.

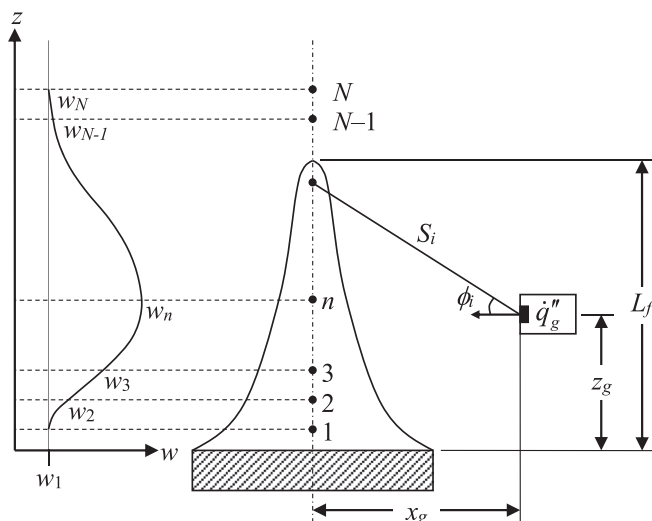


Fig. 1. Geometry setup for the MPS radiation model.

to within 13% for small to medium sized pool fires for measurement locations at separation distances between five and sixteen pool radii. However, it should be noted that measurements at far field locations may not be practical in a laboratory setting and can be affected by resolution issues, due to the marked decrease in heat flux with increasing separation, as well as atmospheric attenuation effects [15].

Hankinson and Lowesmith [16] proposed a weighted multi-point source (MPS) model to determine the radiant fraction of jet flames. This approach was shown to yield reasonably accurate radiant fractions based on both near-field and far-field measurements [16]. Recently, this model has been successfully applied to measure the radiant fraction of buoyant turbulent diffusion line flames [17]. Fig. 1 shows a schematic of the MPS approach, which has been adapted in this study to pool fires. The MPS methodology assumes that N point sources are evenly distributed along the flame axis and the radiation measured by a gage can be calculated as the weighted sum of the radiation from each point source as follows:

$$\dot{q}_g'' = \sum_{i=1}^N w_i \frac{\dot{Q}_r \tau_i}{4\pi S_i^2} \cos \phi_i \quad (3)$$

where w_i is the weight of the i th point source and $\sum w_i = 1$, ϕ_i is the angle between the normal to the gage surface and the line of sight to the i th point source, and τ_i is the transmissivity over the separation distance, S_i , from the i th point source to the gage. The weight profile of the point sources (shown schematically in Fig. 1) was approximated in [16] by a scheme representing weights increasing linearly to a peak at some n th point (where $w_n = n w_1$) and decreasing linearly thereafter so that $w_N = w_1$. It is noted that, for jet flames, the peak weight was positioned at $0.75 L_f$ [16], where L_f is the flame height, based on measurements made on large scale jet fires using a narrow angle radiometer reported by Cook et al. [4], and also the data of Sivathanu and Gore [18] as well as Baillie et al. [19].

The present work applies the MPS model to derive radiant fractions for pool fires burning several liquid fuels with special attention given to the sensitivity of the model to measurement location. To use the MPS model, the radiation distribution must be known so that weights can be assigned (see Fig. 1). Considering the different fire dynamics of jet flames as compared to buoyant turbulent flames, the assumed distribution of jet flames [16] might not be applicable. The only available measured radiation distribution of buoyancy-controlled turbulent diffusion flames reported by Markstein [20] suggests that the distribution is characterized by a slightly asymmetric bell-shaped curve with the maximum occurring at about $0.45 L_f$. However, the gaseous propane fuel used in his study [20] differs from the liquid fuels

considered here. Therefore, rather than presuming a profile, slit radiometer measurements of radiation distribution are part of the present study.

2. Experimental

All the tests were conducted on steady pool fires established in an un-cooled quartz dish of 9.5 cm inner diameter placed in a Fire Propagation Apparatus (FPA) [21,22]. This apparatus provides a calorimetry measurement in an environment with a controlled air co-flow. Dry air was supplied to the system, using a mass flow controller at a flow rate of 100 L/min, through a bed of glass beads to ensure flow uniformity, yielding an upward co-flow of approximately 0.1 m/s. This flow was used to stabilize and anchor the base of the flames and did not alter their buoyant turbulent nature [23,24]. This assumption was verified by varying the flow rate of air without appreciable change (less than 5%) in measured burning rates and radiation profiles.

2.1. Fuel selection

Since sooting propensity is related to the radiant fraction of fuels (e.g., [25]), eleven liquid fuels with different sooting propensities, including alcohols and alkanes, were selected in the present study. The normalized smoke point (NSP) [26] and the net calorific value [27] of each fuel are listed in Table 1. All the fuels used were HPLC grade.

2.2. Fuel supply and level control

The adopted fuel supply system in the present study is similar to that used by Ditch et al. [24]. During the experiment, fuel was continuously fed and controlled with two needle valves connected to a 250 ml burette, as shown in Fig. 2. Fuel dripped through the first needle valve into a burette, which was used to dampen the influence of fuel elevation on the dripping velocity, and then through the second valve into a U-shaped tube connected to the bottom of the quartz dish. Once steady-state conditions were achieved, the mass loss rate (\dot{m}) was calculated based on the average volume change measured by the burette over a given time interval which was usually on the order of 40 min. The uncertainty in \dot{m} is mainly attributed to the manual fuel level control; based on repeated tests, this uncertainty was within 5% for all the used fuels.

2.3. Vertical radiative power distribution measurement

In order to quantify the weight of each point source for use in the MPS model, the slit radiometer methodology developed by Markstein [20] was adopted. As shown in Fig. 2, a horizontal slit from two water-

Table 1
Fuel properties.

Fuel	NSP ^a (mm)	ΔH_{29}^0 (kJ/g) ^b
Methyl alcohol	n.m. ^c	19.94
Ethyl alcohol	n.m.	26.84
n-Propyl alcohol	n.m.	30.71
i-Propyl alcohol	n.m.	30.47
n-Butyl alcohol	n.m.	33.12
n-Amyl alcohol	n.m.	34.79
n-Hexane	149 ± 24	44.74
n-Heptane	139 ± 15	44.56
n-Octane	137 ± 28	44.42
n-Decane	122 ± 14	44.24
Cyclohexane	82 ± 16	43.42

^a Li and Sunderland [26].

^b Values listed are for liquid state and calculated based on standard heat of formation from [27].

^c Not measurable.

Download English Version:

<https://daneshyari.com/en/article/4920978>

Download Persian Version:

<https://daneshyari.com/article/4920978>

[Daneshyari.com](https://daneshyari.com)